Research Square

Preprints are preliminary reports that have not undergone peer review.
They should not be considered conclusive, used to inform clinical practice,
or referenced by the media as validated information.

Shotgun metagenomic profiling of bacterial microbiomes, metagenome-assembled genomes and antimicrobial resistance in respiratory and blood samples from Gambian children with pneumonia

Dam Khan

dam.khan@lshtm.ac.uk

Medical Research Council Unit The Gambia at the London School of Hygiene & Tropical Medicine

Josh L. Espinoza

J. Craig Venter Institute

Peggy-Estelle Tientcheu

Medical Research Council Unit The Gambia at the London School of Hygiene & Tropical Medicine

Isaac Darko Otchere

Noguchi Memorial Institute for Medical Research

Nuredin Ibrahim Mohammed

Medical Research Council Unit The Gambia at the London School of Hygiene & Tropical Medicine

Archibald Worwui

Medical Research Council Unit The Gambia at the London School of Hygiene & Tropical Medicine

Mark P. Nicol

University of Western Australia

Brenda Kwambana-Adams

Liverpool School of Tropical Medicine

Martin Antonio

Medical Research Council Unit The Gambia at the London School of Hygiene & Tropical Medicine

Chris L. Dupont

J. Craig Venter Institute

Article

Keywords: microbiome, metagenome-assembled genomes, antimicrobial resistance, Streptococcus pneumoniae, Haemophilus strains

Posted Date: October 13th, 2026

DOI: https://doi.org/10.21203/rs.3.rs-8724320/v2

License: This work is licensed under a Creative Commons Attribution 4.0 International License.
Read Full License

Additional Declarations: No competing interests reported.

Version of Record: A version of this preprint was published at Scientific Reports on November 12th, 2026. See the published version at https://doi.org/10.1038/s41598-026-80265-y.

Shotgun metagenomic profiling of bacterial microbiomes, metagenome-assembled genomes and antimicrobial resistance in respiratory and blood samples from Gambian children with pneumonia

Dam Khan[1,2] *, Josh L. Espinoza[3], Peggy-Estelle Tientcheu[1], Isaac Darko Otchere[1,4], Nuredin Ibrahim Mohammed[1], Archibald Worwui[1], Mark P. Nicol[5], Brenda Kwambana-Adams[6,7,8], Martin Antonio[1,2,9], and Chris L. Dupont[3]

Author Affiliations

[1]Medical Research Council Unit The Gambia at the London School of Hygiene & Tropical Medicine, Banjul, The Gambia

[2]Department of Infection Biology, Faculty of Infectious and Tropical Diseases, London School of Hygiene & Tropical Medicine, London, United Kingdom

[3]J. Craig Venter Institute, La Jolla, CA, United States of America

[4]Department of Bacteriology, Noguchi Memorial Institute for Medical Research, Legon, University of Ghana, Accra, Ghana

[5]Marshall Centre, Division of Infection and Immunity, School of Biomedical Sciences, University of Western Australia, Perth, Australia

[6]Department of Clinical Sciences, Liverpool School of Tropical Medicine, Liverpool, United Kingdom

[7]Malawi Liverpool Wellcome Programme, Blantyre, Malawi

[8]NIHR Global Health Group on Vaccines to Control Respiratory Pathogens and AMR, Division of Infection and Immunity, University College London, London, United Kingdom

[9]Centre for Epidemic Preparedness and Response, London School of Hygiene & Tropical Medicine, London, United Kingdom

Corresponding author:

Dam Khan

dam.khan@lshtm.ac.uk

Abstract

Pneumonia is a leading cause of morbidity and mortality in children, with bacterial pathogens being important etiologic agents. Most microbiome studies in pneumonia use technologies with limited taxonomical resolution and few include lung aspirate or blood samples. In this study, we assessed the microbial communities of the nasopharynx, nasopharynx/oropharynx, induced sputum, lung aspirate and blood, and recovered metagenome-assembled genomes (MAGs) from the same sites using shotgun metagenomics sequencing of samples from children with severe and very severe pneumonia in The Gambia. Our data show that Proteobacteria and Firmicutes were the most common phyla across the body sites, and this was largely driven by *S. pneumoniae, H. influenzae/aegyptius and M. catarrhalis.* Blood and nasopharyngeal samples showed a mean Jaccard similarity of 58%, which was greater than expected under random pairing of specimens (q = 0.046). We recovered 60 medium-quality MAGs, of which 35 met the criteria for high-quality MAGs including 11 *S. pneumoniae*, 10 *H. influenzae* strains and a *Limosilactobacillus* with less than 95% Average Nucleotide Identity to the closest species in the Genome Taxonomy Database (GTDB). We also showed that antimicrobial resistance genes in our MAGs were highly species-specific; more than 70% of the unique AMR genes detected (11/15) were found only within MAGs of a single bacterial species rather than shared across multiple species. Together, these findings demonstrate the value of shotgun metagenomics in resolving species level detail across clinically relevant but understudied specimen types and provide a genomic resource to support future respiratory pathogen surveillance in low- and middle-income settings.

Keywords: microbiome, metagenome-assembled genomes, antimicrobial resistance, *Streptococcus pneumoniae*, *Haemophilus strains*.

Introduction

Lower respiratory tract infections (LRI) pose a major public health burden and remain one of the main infectious causes of death in low- and middle-income countries[1,2]. LRI, defined by the Global Burden of Disease report as pneumonia or bronchiolitis, was responsible for more than 500,000 deaths in children under five years of age worldwide in 2021[3]. A wide range of organisms cause LRI including bacteria, viruses and fungi. Among the bacterial causes of LRI in 2021, *Streptococcus pneumoniae* was responsible for the highest number of episodes and deaths with an estimated 97·9 million episodes and 505 000 deaths globally across all ages[3]. The risk factors for pneumonia include poverty, malnutrition, lack of exclusive breastfeeding and inadequate vaccination[4,5].

Effective prevention and management strategies for pneumonia, including vaccination and antimicrobials, rely partly on the identification of the microbial etiologic agent of the pneumonia episode, which can be done using culture, nucleic acid amplification, or antigen testing. However, the use of these targeted detection methods limits our understanding of the complex interaction between microbes in the lungs whose interactions affect disease outcome[6]. Samples from the lower respiratory tract are difficult to obtain; therefore, the upper respiratory tract is often studied to gain insights into the microbiome and its role in disease[7]. Understanding the microbiome of the upper respiratory tract is important because it has been postulated that microaspiration is the primary route through which bacteria in the upper airways enter the lungs[8,9], although the temporal, spatial, and regulatory steps that lead to disease are unknown. Moreover, bacterial translocation across the lung epithelium into the blood has also been reported in pneumonia cases[10], highlighting the significance of profiling the microbiome of both the respiratory tract and blood in disease.

The relationship between the upper respiratory airway microbiome and respiratory health is gaining attention[11,12]. For instance, it has been shown that a high abundance of commensal bacterial species

of the *Corynebacterium* and *Dolosigranulum* genera prime the respiratory tract in children through stimulation of innate immunity and competition for resources to restrict colonisation by pathogenic bacteria[13-15]. Conversely, an increased nasopharyngeal density of *S. pneumoniae* may be associated with respiratory illnesses in children[16,17]. This suggests colonisation resistance conferred by protective commensals may be overwhelmed once pathogen density exceeds a critical level tipping the balance from asymptomatic carriage toward symptomatic disease.

Our understanding of the microbiome has traditionally been based on findings from 16S rRNA sequencing technology[18-20]. However, this method lacks species resolution. An untargeted microbial profiling approach, such as shotgun metagenomic sequencing, will provide deeper taxonomical insight into the microbial landscape of the respiratory tract and blood during disease. An added advantage of shotgun metagenomics over 16S rRNA sequencing is its ability to recover metagenome-assembled genomes (MAGs). MAGs are generated by clustering assembled contigs into bins that represent individual organisms, based on nucleotide composition (e.g., tetranucleotide frequency) and coverage patterns across samples[21]. This method has become increasingly important in microbiome research for reconstructing the draft genomes of community members, including uncultured microbes[22-24]. However, many MAGs reported in published studies are of low quality and completeness[24]. Additionally, attempts to recover MAGs from respiratory specimens remain limited. Notably, *Li et al.* constructed a comprehensive respiratory genome catalogue (RGC) of 552 MAGs, although these were derived from only 20 studies[25].

Given the common use of antibiotic regimens in pneumonia patients, profiling antimicrobial resistance genes (AMR) of MAGs in respiratory and blood samples is essential for informing targeted antimicrobial therapy. Moreover, profiling AMR genes contributes to broader efforts in combating antimicrobial resistance which is a global health concern.

Despite the recognised importance of the lower respiratory tract and blood in understanding pneumonia pathogenesis, existing respiratory metagenomic genome catalogues remain built

predominantly from upper respiratory tract specimens across a limited number of studies and populations, with lung aspirate and blood rarely represented and populations from sub-Saharan Africa notably underrepresented. This study addresses t5hese gaps by sampling across five specimen types, including lung aspirate and blood, from a Gambian paediatric pneumonia cohort.

We performed shotgun metagenomics and analysed nasopharyngeal swab (NPS), combined nasopharyngeal and oropharyngeal swabs (NP/OP), induced sputum (IS), lung aspirate (LA), and blood samples from children diagnosed with severe pneumonia to characterise the microbiomes across these sites. Moreover, we aimed to recover MAGs from sample metagenomes of the same specimen types and to characterise their antimicrobial resistance determinants.

Results

Study population demography, clinical features and specimen types

We analysed 71 samples from 37 children hospitalised with pneumonia and who were recruited as part of the PERCH cohort study[26] . The demographic and clinical features of the children are presented in Table 1. The majority were male, 59% (22/37) and 41% (15/37) of the children were less than 6 months old. A total of 54% (20/37) and 51% (19/37) of the cases were fully vaccinated with the *Haemophilus influenzae* type b vaccine and the Pneumococcal Conjugate Vaccine (PCV13) respectively. Very severe pneumonia cases accounted for 57% (21/37) of the cases. NPS comprised the largest proportion of specimens accounting for 41% (29/71) (Supplementary Information, Table S1). Lung aspirates were the least represented sample type with seven specimens. Figure 1 shows specimens analysed from each of the 37 children. Overall, 62% (23/37) of the children provided more than one specimen type. The number of samples analysed in this study was based on availability.

Shotgun metagenomic sequencing depth

Shotgun metagenomic sequencing yielded a median of 19.4 million (Q1-Q3: 4,668,548-22,611,641) reads per sample. No detectable sequencing library was obtained from the blank swab processed during library preparation, and it was therefore not sequenced. The median proportion of reads classified as human-derived was 91.9% (Q1-Q3: 88.3-93.4%). After quality trimming and removal of human reads, the median read count per sample was 1.3 million (Q1-Q3: 802,821-1,693,183). Lung aspirate (median:1,659,428; Q1-Q3: 1,298,046–1,983,546) and blood (median:1,409,762; Q1-Q3: 1,200,388–2,148,311) samples had the highest read depth among the specimen types after quality filtering and removal of human-derived reads. Read depth by specimen type is summarised in Supplementary Information, Table S2.

Metagenomic Assembled Genomes

The MAGs metrices reported follow the Minimum Information about a Metagenome-Assembled Genome (MIMAG) guidelines[27]. A total of 60 Medium-quality MAGs (≥50% completion and <10% contamination) were recovered, of which 35 met the criteria for high-quality MAGs (>90% completeness and <5% contamination) based on MIMAG standards. Details of these 35 high-quality MAGs, including their contamination and completeness as calculated using *CheckM* are provided in Table 2.

Seven species were identified from the 35 high-quality MAGs recovered. These MAGs were obtained from 22 out of 71 samples (31%), and the highest number from a single sample was three. Most MAGs were recovered from blood specimens (11/35, 31%), whereas the fewest were recovered from IS (4/35, 11%). Notably, in 83% (29/35) of the high-quality MAGs, the recovered species corresponded to the species with the highest or second highest relative abundance in the sample from which the MAG was obtained. The number of MAGs recovered by specimen type is described in Supplementary Information, Table S2. Lung aspirate and blood samples showed the highest MAG recovery efficiency when normalised by sample number (1.0 and 1.14 high-quality MAGs per sample

146 respectively, versus 0.21–0.50 for the other three specimen types). The mean number of contigs
147 across all 35 MAGs was 136.2 (Min:22, Max:339), and the mean contig length was 23,934 bp (Min:
148 1500, Max: 472,844). MAG19, which had the lowest number of contigs, had the highest genome
149 completeness at 99.7%.

150 Species assignment of the genomes was based on GTDB-Tk, which integrates average nucleotide
151 identity (ANI) against and phylogenetic placement to assign taxonomy. MAG25 (*Limosilactobacillus*
152 *sp*.) was not assigned a species-level taxonomic classification. The closest match was
153 *Limosilactobacillus gastricus* (GCF_001434365.1), with an ANI of 83.26%. The ANI values for the
154 remaining 42 genetically related *Limosilactobacillus* genomes in the database ranged from 76.2% to
155 78.9% relative to MAG25. The most common species across all MAGs were *S. pneumoniae* (11/35,
156 31%) and *H. influenzae* (10/35, 29%). We obtained MAGs from three unique species of *Moraxella*,
157 including five *M. catarrhalis* MAGs.

158 We performed in silico serotyping and MLST on *S. pneumoniae* and *H. influenzae* MAGs. There was
159 100% concordance between PneumoKITy and SeroBA *S. pneumoniae* serotype assignments. Serotype
160 19A was the most common *S. pneumoniae* serotype (45%, 5/11), as shown in supplementary
161 Information, Table S3. Three of the five serotype 19A strains belonged to the same sequence type
162 (ST847). Three *S. pneumoniae* strains could not be assigned a sequence type on the MLST database.
163 In the only case where we recovered S*. pneumoniae* MAGs from two body sites in the same
164 individual, the strain from blood sample was serotype 19F and ST925, while the strain from NPS was
165 serotype 19A with an unassigned ST. All 10 of the *H. influenzae* strains were non-typeable. Five of
166 them were assigned to distinct sequence types, while the other five could not be assigned a
167 sequence type in the MLST database.

168 A total of 78 AMR genes, including 15 unique genes were detected across the 35 high-quality MAGs
169 (Figure 2A). These genes conferred resistance to eight antibiotic classes. AMR genes conferring
170 resistance to fluoroquinolones were the most prevalent with four unique genes detected, followed

by tetracycline resistance genes which included three unique genes across all MAGs. The average number of AMR genes per MAG was 2.2 (range: 0 – 6) (Figure 2B). Of the nine MAGs with no AMR genes detected, 78% (7/9) were *Haemophilus* species while the remaining two were MAG 25 (*Limosilactobacillus sp.*) from the NP/OP and MAG 35 (*M. lincolnii*) from the NPS.

The AMR genes were largely species specific. Up to 73% (11/15) of the unique AMR genes detected were found only within MAGs of a single bacterial species rather than shared across multiple species. The exceptions were AMR genes *tet(B), tet(R), BRO-1* and *ICR-Mc* each of which was found in MAGs from two different species. In terms of antibiotic class, AMR genes conferring resistance to tetracycline and peptide antibiotic class were present in MAGs of three different species.

Notably, all four *H. influenzae* MAGs from LA carried the *LpsA* gene while none from NPS, NP/OP and IS had the *LpsA* gene. Among the three *H. influenzae* MAGs from blood, two lacked the *LpsA* gene. All 11 *S. pneumoniae* MAGs carried the *patA* and the *patB* genes. The only non-fluoroquinolone or MLS conferring resistance genes in *S. pneumoniae* MAGs were *tet(M)* and *tet(B)* found in blood-derived MAGs. The *ICR-Mc* gene was found in all *M. catarrhalis* MAGs.

We compared the genomic diversity of our high-quality respiratory MAGs against the RGC of *Li et al.*[25] which contains 552 non-redundant medium- and high-quality MAGs using FastANI v1.32. The comparison was restricted to the 24 high-quality MAGs recovered from our respiratory specimens (NPS, NP/OP, IS, LA), as the RGC was derived exclusively from respiratory specimens. In total, 83% (20/24) of our respiratory MAGs shared ≥95% ANI with an existing RGC genome and matched the same species classification (Supplementary Information, Table S4). The remaining four MAGs (17%) that did not meet the ≥95% ANI threshold were MAG1 (*N. meningitidis*), MAG2 (*H. parahaemolyticus*), MAG8 (*H. parahaemolyticus*) and MAG25 (*Limosilactobacillus Sp*.). MAG1 (*N. meningitidis*) shared 85.6% ANI with a Neisseria RGC genome that was not resolved to species level. MAG2 and MAG8 (both *H. parahaemolyticus*) independently matched the same RGC genome

(annotated *Haemophilus parainfluenzae*) sharing 82.6% and 82.8% ANI with it respectively. MAG25 (*Limosilactobacillus sp*) had no detectable hit against any RGC genome.

Microbiome composition of children with pneumonia

All ecological analyses, including relative abundance bar plots, diversity measures, and differential abundance testing, were performed using the species-level cluster (SLC) relative abundance across samples. Each SLC was a cluster of MAGs with ≥95% Average Nucleotide Identity (ANI). The *Haemophilus aegyptius* (a *H. influenzae* biotype) MAG obtained in our dataset clustered at the 95% ANI with *H. influenzae* MAGs. This SLC is designated as *Haemophilus influenzae/aegyptius*. In SLCs that lack species-level classification, the genus name was used along with the SLC identifier as a suffix. To minimize the effects of sequencing noise, taxa with a relative abundance of < 0.1% in any given sample were filtered out from those samples in the analysis.

The mean compositional relative abundance at the phylum and species levels across all samples is shown in Figure 3. The mean compositional relative abundance at the same taxonomic levels for individual samples is shown in Supplementary Information, Figure S1. Overall, the Proteobacteria phylum predominated in IS (66.0%), NPS (63.3%), LA (55.7%) and blood (66.6%) samples. In contrast, Firmicutes was the dominant coloniser in NP/OP samples (46.6%). Bacteroidota and Actinobacteriota contributed less than 5% of the bacterial DNA reads in all specimen types except NP/OP. Fusobacteriota was detected at low mean compositional relative abundance in NPS, NP/OP and IS (0.3% – 0.5%) samples and was absent in LA and blood samples. Patescibacteria (Candidate Phyla Radiation) was detected in one IS sample and one NP/OP sample, with compositional relative abundances of 0.6% and 0.1% respectively in those samples. *S. pneumoniae, H. influenzae/aegyptius* and *M. catarrhalis* consistently had the highest compositional mean relative abundances across all specimen types. *M. catarrhalis* predominated in IS samples with a compositional mean relative abundance of 25.0%; *S. pneumoniae* predominated in NP/OP (29.9%), NPS (26.4%) and LA (40%)

samples. In blood samples, *H. influenzae/aegyptius predominated with* 31.5%. Although *S. pneumoniae, H. influenzae/aegyptius* and *M. catarrhalis* were the most abundant based on the mean relative abundance across specimen types, they were not consistently the most dominant at the individual sample level, except in LA samples, where 57% (4/7) and 43% (3/7) of the samples had *H. influenzae/aegyptius* and *S. pneumoniae* as the dominant species (Supplementary Information, Figure S2). We defined a species as dominant in a sample if it had the highest relative abundance in that sample. In both IS and NP/OP specimens, eight different species dominated across the 12 samples in each group.

We compared Shannon diversity across specimen types using a linear mixed-effects model (Figure 4). The NP/OP samples had the highest diversity (2.13), whereas the LA samples had the lowest diversity (1.19). Pairwise comparison showed significant differences in Shannon diversity between NP/OP and LA ($p = 0.001$), NP/OP and blood ($p = 0.008$), NPS and LA ($p = 0.01$), IS and Blood ($p=0.038$), IS and LA ($p = 0.003$).

We assessed bacterial species overlap between blood and respiratory specimens from the same participants using the Jaccard similarity index (Figure 5). NPS and blood samples from the same participants had a mean Jaccard similarity of 58%, which was greater than the similarity observed under random pairing ($q = 0.046$). In contrast, participant-matched induced sputum and blood samples had mean Jaccard similarity 41%, which did not exceed that expected under random pairing ($q= 0.522$). Similarly, NP/OP and blood samples from the same participants had a mean Jaccard similarity of 34%, with no evidence that similarity exceeded that expected under random pairing ($q= 0.981$).

We restricted our analyses to the nasopharynx and compared the microbial DNA profiles of children with severe and very severe pneumonia. The compositional mean relative abundance of *S. pneumoniae* in the nasopharynx was 33.1% in severe cases and 22.1% in very severe cases (Figure 6). *M. catarrhalis* was detected at a compositional mean relative abundance of 21.3% in severe cases

and 27.5% in very severe cases. The compositional mean relative abundance of *H. influenzae/aegyptius* was similar between the two groups (11.1% in severe cases vs. 11.6% in very severe cases). Notably, the relative abundance of *M. nonliquefaciens* in very severe cases (13.1%) was threefold higher than that in severe cases (3.9%). There was no significant difference in nasopharyngeal Shannon diversity between severe cases and very severe cases (p=0.217), (Supplementary Information, Figure S3). In addition, the multivariable model found no significant association in nasopharyngeal Shannon diversity between severe cases and very severe cases (p=0.069). Furthermore, PERMANOVA detected no significant difference in nasopharyngeal microbiome composition between the two groups (P=0.634), Supplementary Information, Figure S4. MaAsLin3 differential abundance testing of nasopharyngeal samples yielded no significant associations between bacterial species and pneumonia severity classification. We compared the relative abundance of *S. pneumoniae* between children with full (n=14) versus incomplete PCV vaccination status (n=13), as well as *H. influenzae/aegyptius* relative abundance between children with full (n=15) versus incomplete Hib vaccination status (n=12) in the nasopharynx of the children. *S. pneumoniae* relative abundance was similar between fully and incompletely PCV-vaccinated children (mean relative abundance: 27.5% vs. 27.8%; q = 0.519). *H. influenzae/aegyptius* relative abundance was lower in fully Hib-vaccinated children compared to those incompletely vaccinated (mean relative abundance: 7.1% vs. 13.6%), although this difference was not statistically significant after correction for multiple testing (q = 0.106).

Discussion

Few studies have characterised the respiratory or blood microbiome in children with pneumonia in such detail. Using shotgun metagenomics in this study, we found *S. pneumoniae*, *H. influenzae/aegyptius* and *M. catarrhalis* were the most common species from all sample types. Furthermore, we observed greater species overlap between blood and nasopharyngeal samples from the same participants than expected under random pairing. A major strength of our work lies in the

recovery of 35 high-quality MAGs in these niches, including what appears to be a novel *Limosilactobacillus* with less than 95% ANI to any species in GTDB.

Our analysis of the microbial profile of the respiratory tract and blood during infection achieved species-level resolution which is seldom achieved in respiratory microbiome studies. Proteobacteria and Firmicutes dominated in the respiratory samples, and this was largely driven by *S. pneumoniae*, *H. influenzae* and *M. catarrhalis*. These are clinically important pathogens, and vaccines targeting *S. pneumoniae* and *H. influenzae* type b are routinely administered in many countries including The Gambia[28-30]. Our findings are consistent with other studies in The Gambia where *S. pneumoniae* and *H. influenzae* were identified as the primary bacterial pathogens causing pneumonia in children, based on microbiology culture and PCR analyses of lung and pleural aspirates[31]. The high prevalence of *S. pneumoniae* detected in our analysis is also consistent with previous reports from The Gambia where carriage rates among children under one year of age were as high as 97%[32]. Although the introduction of Pneumococcal Conjugate Vaccines (PCVs) has led to the reduction of vaccine-type carriage, the overall carriage of *S. pneumoniae* remains unchanged. The reason for this persistence is likely due to the increase in the carriage of non-vaccine serotypes[33].

S. pneumoniae serotype 19A was the most common serotype in our dataset among the high-quality MAGs we recovered. This serotype increased in prevalence in many countries following the introduction of the seven valent pneumococcal vaccine (PCV7)[34]. ST847 was the most frequently observed assigned sequence type in our dataset and has been associated with serotype 19A in both carriage[35] and disease[36]. *H. influenzae* type b (Hib) disease and carriage have declined globally due to the introduction of the Hib vaccine[37,38]. However, non-typeable *H. influenzae* which was the most common *H. influenzae* type recovered among our high-quality MAGs, has been reported elsewhere as responsible for the majority of otitis media, sinusitis, and pneumonia cases among children vaccinated with the Hib vaccine[39].

In our analysis, there were no significant differences in nasopharyngeal microbiome diversity between severe and very severe cases. Differential abundance testing also revealed no significant differences in any species by case type. This finding may reflect our small sample size limitation. Previous studies have reported that the upper respiratory tract microbiome composition can serve as a marker for severity of lower respiratory tract disease[40].

It is traditionally understood that the blood is sterile, largely from the fact that the presence of bacteria as low as 1-10 bacterial cells per millilitre of whole blood is potentially life threatening[41]. However, there is growing evidence that bacterial DNA of various taxa can be detected in blood driven by 16S or shotgun sequencing [42-44]. It remains unclear whether bacterial DNA detected in blood represents viable organisms or remnants, and whether these arise from leakages from other body sites. Proteobacteria, Firmicutes and Actinobacteria have been reported as predominant phyla in blood across various conditions and age group[45-47]. Consistently, our analysis of children with pneumonia revealed a similar dominance of the same phyla.

The fact that DNA from many different bacterial taxa can be detected in blood poses a problem in using bacterial reads from metagenomic sequencing in determining etiology. *Barbeta, E. et al.* found 21 Operational Taxonomic Units in sixteen blood samples, even though only fifteen percent of those samples had positive blood culture[48]. A key finding from our study is that nasopharyngeal and blood samples from the same individuals shared greater species overlap than expected under random pairing. This participant-specific similarity was specific to the NPS–blood comparison, as the overlap between induced sputum and blood and between NP/OP and blood did not exceed that observed under random pairing. Whether the observed NPS–blood similarity reflects biological continuity between the upper respiratory tract and bloodstream, or other factors influencing the detection of bacterial DNA in blood, warrants further investigation

We conducted a comprehensive sample level recovery of metagenomes resulting in the identification of 35 MAGs that met the MIMAG criteria for high-quality genomes. This was achieved using

consensus binning, a very stringent approach that leverages the strengths of the different binning algorithms (MaxBin2, MetaBAT2 and CONCOCT) while minimising their individual limitations. This strategy recovered high-quality bins that would have been missed by using a single algorithm alone. However, the relatively limited microbial sequencing depth after host-read removal may have constrained assembly and MAG recovery, particularly for low-abundance organisms. The 35 high-quality MAGs recovered in this study are therefore not an exhaustive representation of the microbial communities present in these specimens.

Recovery of MAGs from metagenomes enhances the identification of organisms that are not routinely targeted for disease diagnostic purposes by other methods such as PCR. Furthermore, it is a valuable for identifying species that are difficult to culture in the lab. Notably, we recovered a high-quality genome belonging to the *limosilactobacillus* genus that did not meet the 95% ANI threshold for species-level assignment in the Genome Taxonomy Database. An ANI range of 95–96% is commonly used to delineate species boundary[49,50]. *Limosilactobacillus* is a genus within the family Lactobacillaceae. It was formally classified as lactobacillus until a reclassification in 2020 divided lactobacillus into 25 novel genera including *Limosilactobacillus*[51]. To date, up to 23 species of *Limosilactobacillus* have been described in both human and non-human hosts[52]. Our *Limosilactobacillus sp.* MAG was recovered from the NP/OP, and it potentially represents a previously undescribed or novel species within this genus.

To further contextualise the diversity of our recovered genomes, we compared our respiratory MAGs against the Respiratory Genome Catalogue[25]. While the majority (83%) of our respiratory MAGs closely matched existing catalogued genomes, four of our MAGs were not represented in the catalogue suggesting that, despite expected overlap with well-characterised respiratory taxa, our dataset contributed additional genomic representation. This underscores the value of sampling underrepresented populations.

While we used *checkM* metrics to ascertain the quality of our genomes, some studies have raised concern that the quality of MAGs may be overestimated by commonly used pipelines for assessing genome quality. *Meziti et al.*[53] explored this by comparing gene variability between pathogenic *Escherichia coli* isolates from diarrheal samples against their corresponding MAGs recovered from the same samples. Their analysis showed that completeness estimates near 95% as reported by the *MiGA* workflow captured only 77% of the population core genes and 50% of the variable genes. They were also able to find that about 5% of the genes from the MAGs were missing in the isolate and were of different taxonomic origin, even though pipeline-based contamination estimates were as low as 1.5%. However, these findings were based on a single bacterial species and may not apply to the species present in our dataset. *Meziti et al*. further outlined key criteria that contributes to MAGs reliability beyond standard pipeline-based completeness and contamination estimates. These include MAGs having fewer than 500 contigs, contig lengths greater than 1000 bp, N50 values above 20,000 bp and genome size deviations less than 0.5 Mb compared to reference strains. Our high-quality genomes meet these benchmarks in terms of contig number, contig length, genome size consistency. Additionally, more than 60% of our MAGs had N50 values exceeding 20,000 bp further supporting the overall high-quality of our MAGs. However, we still would recommend conducting gene content comparison and SNP analysis between paired *S. pneumoniae* isolate and MAG strains obtained from the same sample. This will be crucial for assessing the reliability of using sample driven *S. pneumoniae* MAGs for public health applications such as tracking vaccine impacts and in outbreak investigations. What we have not been able to achieve is the recovery of multiple high-quality MAGs of the same species from a single sample. In each case, only one strain of a single species is successfully binned. This limitation is particularly important for *S. pneumoniae* where multiple strain carriage in the upper respiratory tract is common[54,55]. Co-carriage was observed in 15% of children in South Africa[56] using shotgun metagenomics sequencing and more than 48% of children in Southeast Asia by microarray[57]. In our upper respiratory tract samples where *S. pneumoniae* was recovered, it is possible that more than one strain was present in some samples but only one dominant strain was

recovered. This suggests that our sequencing procedure or sample-specific binning procedures are limited in their ability to recover co-existing strains of the same species in a sample. The only pair of *S. pneumoniae* MAGs recovered from blood and NPS of the same individual belonged to different serotypes and sequence types. This highlights that using MAGs to study strain-level similarity of *S. pneumoniae* across body sites may be unreliable.

While the presence of an AMR genes does not equate to clinical resistance, monitoring their presence in the respiratory tract and blood could provide insights into which antibiotics the bacteria are resistant to. Additionally, given that some AMR genes can be transferred to other bacterial species in the same niche through horizontal gene transfer, it is important to identify which genes have the potential to spread to other bacteria. The *patA* and *patB* AMR genes were highly prevalent in our *S. pneumoniae* MAGs. These genes interact to form an ATP-binding cassette (ABC) antibiotic efflux pump that confers resistance to fluoroquinolones in *S. pneumoniae*[58,59]. Resistance to the common fluoroquinolone, ciprofloxacin in *S. pneumoniae* mainly occurs through the acquisition of mutations in the quinolone resistance-determining region of the *ParC* and *gyrA* genes. However, *Lupien et al.* have shown that the *patA* and *patB* genes also contribute to low-level resistance to ciprofloxacin in a clinical isolate[60]. The analysis we carried out on the CARD database couldn't infer penicillin resistance due to PBP mutations. Future analyses could complement CARD-based genotypic screening with CDC PBP-based pipeline to infer penicillin-binding protein-mediated β-lactam resistance phenotypes. *M. catarrhalis* is among the species that are intrinsically resistant to colistin. The ICR-Mc gene found in our *M. catarrhalis* MAGs encodes a chromosomally located colistin resistance phosphoethanolamine (PEtN) transferase[61]. The protein is the closest known ortholog to the well-known plasmid mediated colistin resistance genes *mcr-1* and *mcr-2*[61]. The *LpsA* gene was detected in *H. influenzae* MAGs in LA but absent in MAGs from NP/OP, NPS and IS. *LpsA* confers intrinsic resistance to peptide antibiotics[62] but it is more widely known for its role in lipooligosaccharide biosynthesis[63] and it has been associated with adaptation to the lung environment and invasiveness[64]

A major limitation of our study was the sample size which limited statistical power and the generalisability of some of our findings. Secondly, we did not obtain controls at the sampling point to control for contamination during sampling. Controls at the DNA extraction stage were also not available for sequencing. Therefore, contamination introduced during sample collection or DNA extraction could not be directly assessed. However, we reduced the potential influence of taxa commonly associated with skin contamination by excluding *Cutibacterium acnes, Staphylococcus saprophyticus* and *Staphylococcus epidermidis* from all samples in this analysis. This decision was made because these bacteria primarily colonise the skin and not the specimen types we analysed and could have contaminated our samples during sample collection. They have also been implicated as contaminants in microbiome studies of low-biomass samples[41,65]. A further limitation in the DNA extraction method was the confounding with specimen type. Because extraction kit and specimen type did not vary independently in this study, we could not statistically disentangle the effects of extraction method from those of specimen type. Consequently, differences in microbial composition may partly reflect differences in DNA extraction efficiency rather than biological differences between anatomical sites. The use of different extraction protocols was necessary to accommodate the distinct specimen matrices and their respective processing requirements, but this limits direct comparisons of microbial composition across specimen types. Future studies designed to compare microbial communities across specimen types should include appropriate cross-extraction controls to quantify methodological effects. Thirdly, blood, NP/OP, and induced sputum specimens were analysed exclusively from patients with very severe disease, resulting in strong confounding between specimen type and disease severity. Therefore, observed differences in microbial diversity between specimen types should be interpreted cautiously as they may reflect differences in disease severity rather than anatomical site alone. Fourth, a few children were administered antibiotics before sample collection, and this could have impacted their microbiome profiles. The fifth limitation was the substantial proportion of host-derived reads following microbial DNA enrichment. The relatively limited microbial sequencing depth may have constrained assembly and MAG recovery, particularly

for low-abundance organisms. Additionally, pre-enrichment sequencing was not performed. Therefore, we could not directly quantify the efficiency of the microbial DNA enrichment procedure or determine the reduction in host-derived DNA attributable to the enrichment step. Finally, our analysis could not establish whether the relative abundances of the different species in our samples reflected the existence of viable bacteria or bacteria-derived DNA. Therefore, the bacterial profiles of samples may not represent the viable microbiome at the time of sample collection, and as such our findings should be interpreted with caution.

Conclusion

Despite our limitations, we have been able to show that overall, the bacterial DNA from *S. pneumoniae, H. influenzae/aegyptius* and *M. catarrhalis* were the most common across the different body sites we studied in children with pneumonia in The Gambia. We also found greater bacterial species similarity between nasopharyngeal and blood samples from the same participants than expected under random pairing, suggesting a participant-specific signal in the bacterial DNA detected across these specimens. Thirdly, we have been able to recover high-quality MAGs from our samples further advancing the field of genomics of important pathogens like *H. influenzae and S. pneumoniae.* For future studies, it is essential to include sampling controls that undergo the same sequencing procedure as the samples. We also propose future studies in metatranscriptomics to study the activities of live bacteria present in blood and respiratory samples of pneumonia patients. Finally, we propose comparing MAGs and isolates of *S. pneumoniae* strains from the same respiratory or blood sample to assess how well the MAG genome reflects that of the isolate.

Methods

Study participants and sample collection

We used stored samples obtained between 2011 and 2014 from participants recruited in the Pneumonia Etiology Research for Child Health (PERCH) study[26]. PERCH was a case-control study that sought to characterise the causes of severe childhood pneumonia in children living in high pneumonia burden and low-resource regions, including The Gambia. The samples analysed in this study were exclusively from children with pneumonia. In the PERCH study, children aged 1-59 months who presented and were admitted to the hospital in Basse, Upper River Region of The Gambia, with severe or very severe pneumonia were recruited. Severe pneumonia was defined as cough or difficulty breathing with lower chest wall indrawing, and very severe pneumonia was defined as cough or difficulty breathing and at least one of the following signs: vomiting everything, difficulty in drinking or breastfeeding, central cyanosis, lethargy, convulsions, unconsciousness, or head-nodding. Specimens, including NPS, NP/OP swabs, blood, IS and LA, were collected at enrolment. NPS were collected and stored as a distinct specimen. Separately, NP/OP specimen was collected by combining a second nasopharyngeal swab with an oropharyngeal swab into a single collection tube. Further details on participant recruitment, sample collection rationale, case definitions, inclusion criteria of the PERCH study are described elsewhere[26,66].

Ethics

Ethical approval for the Gambian samples used in the PERCH study was obtained from the Johns Hopkins Bloomberg School of Public Health Institutional Review Board (JHSPH IRB), and local ethical approval was obtained from the Joint MRC Unit The Gambia at The London School of Hygiene and Tropical Medicine and The Government of The Gambia Ethics Committee. Written informed consent was obtained from the patient's guardians for all procedures performed in the study. All procedures were performed in accordance with relevant guidelines and regulations.

Laboratory procedures

DNA was extracted from all samples using QIAGEN kits at the molecular diagnostics laboratory at the Medical Research Council unit The Gambia at the London School of Hygiene and Tropical Medicine,

based in The Gambia following the manufacturer's instructions. The laboratory is subscribed to the UK NEQAS External Quality Assessment (EQA) provider. DNA extraction methods differed according to specimen matrix. Total DNA was extracted from the stored NPS, NP/OP, and IS samples using the DNeasy PowerSoil Kit[67], whereas DNA from the LA and blood samples was extracted using the QIAamp MinElute Virus Spin kit[68] and the QiAamp DNA Blood Mini Kit[69], respectively. Library preparation and sequencing of the samples were carried out at the John Craig Venter Institute, San Diego, US. Firstly, extracted DNA samples were enriched for microbial DNA using the NEBNext Microbiome DNA kit (New England Biolabs) following the manufacturer's instructions before whole metagenomic sequencing using the Illumina NovaSeq 2X150bp. DNA extraction controls were not available for sequencing. Blank controls (sterile swabs) were included throughout the library preparation process to monitor for contamination in the laboratory reagents.

Sequencing reads processing

Preprocessing of reads, and the recovery, taxonomic classification and quality assessment of MAGs were performed using modules in the Viral (micro) Eukaryotic Bacterial Archaeal (VEBA) open-source software suite, v1.0.2a[70,71]. Within VEBA's *preprocess.py* module, adapter removal and quality trimming were carried out using fastp v0.23.2[72], and pairing of the trimmed reads was assessed and corrected using BBTools v38.92[73]. Sequencing reads were mapped to the T2T-CHM13v2.0 human reference genome using Bowtie2 v2.3.5.1[74]. All reads aligning to this reference were classified as human-derived and removed prior to downstream analysis. Cleaned reads were input into VEBA's *assembly.py* module, where they were assembled using metaSPAdes (SPAdes suite, v3.15.3)[75]. Binning was performed using MetaBAT2 v2.15[76], CONCOCT v1.1.0[77] and MaxBin2 v2.2.7[78], followed by DAS Tool v1.1.2[79]for consensus binning. MAGs were quality assessed by CheckM v1.1.3[80]. The genome statistics such as N50, number of contigs and genome size were calculated using *SeqKit* v2.0.0[81]. Taxonomic classification of the genomes was performed using the Genome Taxonomy

Database Toolkit *GTDB-TK*[82] v2.1.1 with GTDB release R207v2, based on sequence similarity (FASTANI) and phylogenetic placement.

MAGs with ≥95% Average Nucleotide Identity (ANI) were clustered into SLCs using VEBA's *cluster.py* module. Sequencing reads were mapped to SLC representative genomes, and contig-level counts were generated using *featureCounts* as part of the VEBA workflow. For samples with unbinned contigs, pseudo- coassemblies were created to enable additional binning and taxonomic assignment.

S. pneumoniae and _H. influenzae_ serotyping and Multi-Locus Sequence Typing

FASTA files from *S. pneumoniae* MAGs were analysed using PneumoKITy v1.0[83] to assign in silico *S. pneumoniae* serotypes. SeroBA (v2.0.4)[84] was used to cross-validate the PneumoKITy serotype assignments. In silico serotyping of *H. influenzae* MAGs was performed using hicap v1.0.3[85]. Multi-locus sequence types for both *S. pneumoniae* and *H. influenzae* were assigned using PubMLST[86]. The seven housekeeping genes analysed for *S. pneumoniae* were: *aroE, ddl, gdh, gki, recP, spi,* and *xpt.* For *H. influenzae,* the seven genes were: *adk, atpG, frdB, fucK, mdh*, *pgi* and *recA*

Antimicrobial Resistance determinants for MAGs

The recovered MAGs were submitted to the Comprehensive Antimicrobial Resistance Database (CARD) to identify and annotate AMR genes. Only AMR gene hits classified under "perfect" or "strict" categories and a cutoff of >90% sequence identity of the matching region were considered.

Statistical analysis

Statistical analysis and visualisation were conducted using Rstudio v4.4.2. Shannon diversity indices were compared across specimen types using a linear mixed-effects model with specimen type as a fixed effect and participant as a random intercept to account for repeated sampling of the same children across multiple specimen types. Pairwise comparisons between specimen types were derived from the fitted model using estimated marginal means and Tukey's method was applied to adjust for multiple comparisons.

We calculated the Jaccard similarity index to quantify bacterial species overlap between paired blood and respiratory samples from the same participants. In addition, we performed a permutation test to generate a null distribution. The null hypothesis was that participant-matched samples were no more similar than randomly paired samples. For each permutation, we randomly shuffled the specimens of one type across participants while keeping the specimens of the other type fixed, thereby breaking the original participant-level pairing. We recalculated the mean Jaccard similarity for each permutation and repeated this procedure 9,999 times to generate the null distribution. We calculated one-sided P values as the proportion of permuted mean similarities that were greater than or equal to the observed mean similarity. We performed separate tests for NPS versus blood, induced sputum versus blood, and NP/OP versus blood. We used the Benjamini–Hochberg procedure to control for false discovery rate and $q < 0.05$ was considered significant.

We evaluated differences in Shannon diversity between the nasopharynx of severe cases and very severe cases using a two tailed Mann-Whitney U test. In addition, a multivariable linear model of Shannon diversity with disease severity, age and PCV vaccination as covariates was fitted as a sensitivity analysis. We computed the Aitchison distance (i.e., Euclidean distance on the centred log-ratio transformed data) and used principal coordinates analysis (PCoA) to plot the beta diversity of the nasopharynx in severe and very severe cases. Permutational multivariate analysis of variance (PERMANOVA) was performed to determine whether beta diversity differed between the two groups adjusting for age and vaccination status. Differences in *S. pneumoniae* relative abundance between fully PCV vaccinated and incompletely vaccinated children (combining partial and no vaccination) were restricted to nasopharyngeal swab (NPS) samples and evaluated using the two-tailed Mann-Whitney U test. A similar analysis was carried out to test for differences in *H. influenzae* relative abundance between fully Hib vaccinated and incompletely vaccinated children. P values were adjusted using the Benjamini-Hochberg (q) false discovery rate correction. A significance threshold of $q < 0.05$ was used.

546 We used Microbiome Multivariable Associations with Linear Models (MaAsLin3 v 0.99.2)[87] to
547 identify differences in microbial species between the nasopharynx of severe cases and very severe
548 cases. Abundance data were normalised using centred log-ratio (CLR) transformation implemented in
549 MaAsLin3, with zero values handled internally by the package. Species were filtered to those
550 detected in at least 15% of samples prior to model fitting to ensure adequate non-zero observations
551 for stable effect estimation. Age was included as a covariate in the model, and all associations were
552 considered significant at an FDR-corrected q-value threshold of 0.1, consistent with MaAsLin3
553 default.

554 All figures in the manuscript were generated using ggplot2 v 4.0.3 and microViz v 0.12.6[88].

555
556
557
558
559
560
561
562
563
564
565
566
567
568
569
570
571
572
573

References

1 Liu, L. *et al.* Global, regional, and national causes of under-5 mortality in 2000-15: an updated systematic analysis with implications for the Sustainable Development Goals. *Lancet* **388**, 3027-3035 (2016). https://doi.org:10.1016/s0140-6736(16)31593-8

2 Walker, C. L. F. *et al.* Global burden of childhood pneumonia and diarrhoea. *Lancet* **381**, 1405-1416 (2013). https://doi.org:10.1016/s0140-6736(13)60222-6

3 Global, regional, and national incidence and mortality burden of non-COVID-19 lower respiratory infections and aetiologies, 1990-2021: a systematic analysis from the Global Burden of Disease Study 2021. *Lancet Infect Dis* **24**, 974-1002 (2024). https://doi.org:10.1016/s1473-3099(24)00176-2

4 Goyal, J. P. *et al.* Risk Factors for the Development of Pneumonia and Severe Pneumonia in Children. *Indian Pediatr* **58**, 1036-1039 (2021).

5 Nguyen, T. K. *et al.* Risk factors for child pneumonia - focus on the Western Pacific Region. *Paediatr Respir Rev* **21**, 95-101 (2017). https://doi.org:10.1016/j.prrv.2016.07.002

6 Pirrone, M., Pinciroli, R. & Berra, L. Microbiome, biofilms, and pneumonia in the ICU. *Curr Opin Infect Dis* **29**, 160-166 (2016). https://doi.org:10.1097/qco.0000000000000255

7 Kumpitsch, C., Koskinen, K., Schöpf, V. & Moissl-Eichinger, C. The microbiome of the upper respiratory tract in health and disease. *BMC Biol* **17**, 87 (2019). https://doi.org:10.1186/s12915-019-0703-z

8 Dickson, R. P. *et al.* Bacterial Topography of the Healthy Human Lower Respiratory Tract. *mBio* **8**, 10.1128/mbio.02287-02216 (2017). https://doi.org:doi:10.1128/mbio.02287-16

9 Mitsi, E. *et al.* Nasal Pneumococcal Density Is Associated with Microaspiration and Heightened Human Alveolar Macrophage Responsiveness to Bacterial Pathogens. *Am J Respir Crit Care Med* **201**, 335-347 (2020). https://doi.org:10.1164/rccm.201903-0607OC

10 Bhowmick, R. *et al.* Systemic Disease during Streptococcus pneumoniae Acute Lung Infection Requires 12-Lipoxygenase–Dependent Inflammation. *The Journal of Immunology* **191**, 5115-5123 (2013). https://doi.org:10.4049/jimmunol.1300522

11 de Steenhuijsen Piters, W. A., Sanders, E. A. & Bogaert, D. The role of the local microbial ecosystem in respiratory health and disease. *Philos Trans R Soc Lond B Biol Sci* **370** (2015). https://doi.org:10.1098/rstb.2014.0294

12 Camelo-Castillo, A. *et al.* Nasopharyngeal Microbiota in Children With Invasive Pneumococcal Disease: Identification of Bacteria With Potential Disease-Promoting and Protective Effects. *Front Microbiol* **10**, 11 (2019). https://doi.org:10.3389/fmicb.2019.00011

13 Biesbroek, G. *et al.* Early respiratory microbiota composition determines bacterial succession patterns and respiratory health in children. *Am J Respir Crit Care Med* **190**, 1283-1292 (2014). https://doi.org:10.1164/rccm.201407-1240OC

14 Stubbendieck, R. M., Hurst, J. H. & Kelly, M. S. Dolosigranulum pigrum: A promising nasal probiotic candidate. *PLoS Pathog* **20**, e1011955 (2024). https://doi.org:10.1371/journal.ppat.1011955

15 Raita, Y. *et al.* Maturation of nasal microbiota and antibiotic exposures during early childhood: a population-based cohort study. *Clin Microbiol Infect* **27**, 283.e281-283.e287 (2021). https://doi.org:10.1016/j.cmi.2020.05.033

16 Chochua, S. *et al.* Increased Nasopharyngeal Density and Concurrent Carriage of Streptococcus pneumoniae, Haemophilus influenzae, and Moraxella catarrhalis Are Associated with Pneumonia in Febrile Children. *PLoS One* **11**, e0167725 (2016). https://doi.org:10.1371/journal.pone.0167725

17 Fan, R. R. *et al.* Nasopharyngeal Pneumococcal Density and Evolution of Acute Respiratory Illnesses in Young Children, Peru, 2009-2011. *Emerg Infect Dis* **22**, 1996-1999 (2016). https://doi.org:10.3201/eid2211.160902

18 Xu, L., Earl, J. & Pichichero, M. E. Nasopharyngeal microbiome composition associated with Streptococcus pneumoniae colonization suggests a protective role of Corynebacterium in young children. *PLoS One* **16**, e0257207 (2021). https://doi.org:10.1371/journal.pone.0257207

19 de Steenhuijsen Piters, W. A. A. *et al.* Interaction between the nasal microbiota and S. pneumoniae in the context of live-attenuated influenza vaccine. *Nat Commun* **10**, 2981 (2019). https://doi.org:10.1038/s41467-019-10814-9

20 Kelly, M. S. *et al.* Non-diphtheriae Corynebacterium species are associated with decreased risk of pneumococcal colonization during infancy. *Isme j* **16**, 655-665 (2022). https://doi.org:10.1038/s41396-021-01108-4

21 Han, H., Wang, Z. & Zhu, S. Benchmarking metagenomic binning tools on real datasets across sequencing platforms and binning modes. *Nat Commun* **16**, 2865 (2025). https://doi.org:10.1038/s41467-025-57957-6

22 León, M. J. *et al.* From metagenomics to pure culture: isolation and characterization of the moderately halophilic bacterium Spiribacter salinus gen. nov., sp. nov. *Appl Environ Microbiol* **80**, 3850-3857 (2014). https://doi.org:10.1128/aem.00430-14

23 Stewart, R. D. *et al.* Compendium of 4,941 rumen metagenome-assembled genomes for rumen microbiome biology and enzyme discovery. *Nat Biotechnol* **37**, 953-961 (2019). https://doi.org:10.1038/s41587-019-0202-3

24 Almeida, A. *et al.* A new genomic blueprint of the human gut microbiota. *Nature* **568**, 499-504 (2019). https://doi.org:10.1038/s41586-019-0965-1

25 Li, Y. *et al.* Comprehensive human respiratory genome catalogue underlies the high resolution and precision of the respiratory microbiome. *Briefings in Bioinformatics* **26** (2024). https://doi.org:10.1093/bib/bbae620

26 Causes of severe pneumonia requiring hospital admission in children without HIV infection from Africa and Asia: the PERCH multi-country case-control study. *Lancet* **394**, 757-779 (2019). https://doi.org:10.1016/s0140-6736(19)30721-4

27 Bowers, R. M. *et al.* Minimum information about a single amplified genome (MISAG) and a metagenome-assembled genome (MIMAG) of bacteria and archaea. *Nat Biotechnol* **35**, 725-731 (2017). https://doi.org:10.1038/nbt.3893

28 Wahl, B. *et al.* Burden of Streptococcus pneumoniae and Haemophilus influenzae type b disease in children in the era of conjugate vaccines: global, regional, and national estimates for 2000-15. *Lancet Glob Health* **6**, e744-e757 (2018). https://doi.org:10.1016/s2214-109x(18)30247-x

29 Zaman, S. M. *et al.* Impact of routine vaccination against Haemophilus influenzae type b in The Gambia: 20 years after its introduction. *J Glob Health* **10**, 010416 (2020). https://doi.org:10.7189/jogh.10.010416

30 Mackenzie, G. A. *et al.* A cluster-randomised, non-inferiority trial of the impact of a two-dose compared to three-dose schedule of pneumococcal conjugate vaccination in rural Gambia: the PVS trial. *Trials* **23**, 71 (2022). https://doi.org:10.1186/s13063-021-05964-5

31 Howie, S. R. *et al.* Etiology of severe childhood pneumonia in the Gambia, West Africa, determined by conventional and molecular microbiological analyses of lung and pleural aspirate samples. *Clin Infect Dis* **59**, 682-685 (2014). https://doi.org:10.1093/cid/ciu384

32 Hill, P. C. *et al.* Nasopharyngeal carriage of Streptococcus pneumoniae in Gambian villagers. *Clin Infect Dis* **43**, 673-679 (2006). https://doi.org:10.1086/506941
33 Kwambana-Adams, B. *et al.* Rapid replacement by non-vaccine pneumococcal serotypes may mitigate the impact of the pneumococcal conjugate vaccine on nasopharyngeal bacterial ecology. *Sci Rep* **7**, 8127 (2017). https://doi.org:10.1038/s41598-017-08717-0
34 Ruiz García, Y. *et al.* CIRCULATING CLONAL COMPLEXES AND SEQUENCE TYPES OF STREPTOCOCCUS PNEUMONIAE SEROTYPE 19A WORLDWIDE: THE IMPORTANCE OF MULTIDRUG RESISTANCE: A SYSTEMATIC LITERATURE REVIEW. *Expert Rev Vaccines* **20**, 45-57 (2021). https://doi.org:10.1080/14760584.2021.1873136
35 Roca, A. *et al.* Nasopharyngeal carriage of pneumococci four years after community-wide vaccination with PCV-7 in The Gambia: long-term evaluation of a cluster randomized trial. *PLoS One* **8**, e72198 (2013). https://doi.org:10.1371/journal.pone.0072198
36 Li, T. *et al.* Pan-Genome-Wide Association Study of Serotype 19A Pneumococci Identifies Disease-Associated Genes. *Microbiol Spectr* **11**, e0407322 (2023). https://doi.org:10.1128/spectrum.04073-22
37 Slack, M. *et al.* Haemophilus influenzae type b disease in the era of conjugate vaccines: critical factors for successful eradication. *Expert Rev Vaccines* **19**, 903-917 (2020). https://doi.org:10.1080/14760584.2020.1825948
38 Yang, Y. *et al.* Haemophilus influenzae type b carriage and burden of its related diseases in Chinese children: Systematic review and meta-analysis. *Vaccine* **35**, 6275-6282 (2017). https://doi.org:10.1016/j.vaccine.2017.09.057
39 Khattak, Z. E. & Anjum, F. in *StatPearls* (StatPearls Publishing

Copyright © 2025, StatPearls Publishing LLC., 2025).

40 Teo, S. M. *et al.* The infant nasopharyngeal microbiome impacts severity of lower respiratory infection and risk of asthma development. *Cell Host Microbe* **17**, 704-715 (2015). https://doi.org:10.1016/j.chom.2015.03.008
41 Whittle, E., Leonard, M. O., Harrison, R., Gant, T. W. & Tonge, D. P. Multi-Method Characterization of the Human Circulating Microbiome. *Front Microbiol* **9**, 3266 (2018). https://doi.org:10.3389/fmicb.2018.03266
42 Castillo, D. J., Rifkin, R. F., Cowan, D. A. & Potgieter, M. The Healthy Human Blood Microbiome: Fact or Fiction? *Front Cell Infect Microbiol* **9**, 148 (2019). https://doi.org:10.3389/fcimb.2019.00148
43 Schierwagen, R. *et al.* Circulating microbiome in blood of different circulatory compartments. *Gut* **68**, 578-580 (2019). https://doi.org:10.1136/gutjnl-2018-316227
44 Potgieter, M., Bester, J., Kell, D. B. & Pretorius, E. The dormant blood microbiome in chronic, inflammatory diseases. *FEMS Microbiol Rev* **39**, 567-591 (2015). https://doi.org:10.1093/femsre/fuv013
45 Amar, J. *et al.* Blood microbiota dysbiosis is associated with the onset of cardiovascular events in a large general population: the D.E.S.I.R. study. *PLoS One* **8**, e54461 (2013). https://doi.org:10.1371/journal.pone.0054461
46 Liu, W. *et al.* Characterization of blood and urine microbiome temporal variability in patients with acute myeloid leukemia. *Microb Pathog* **206**, 107734 (2025). https://doi.org:10.1016/j.micpath.2025.107734
47 Khan, I. *et al.* Analysis of the blood bacterial composition of patients with acute coronary syndrome and chronic coronary syndrome. *Front Cell Infect Microbiol* **12**, 943808 (2022). https://doi.org:10.3389/fcimb.2022.943808
48 Barbeta, E. *et al.* Biological effects of pulmonary, blood and gut microbiome alterations in patients with acute respiratory distress syndrome. *ERJ Open Res* **11** (2025). https://doi.org:10.1183/23120541.00667-2024

49 Riesco, R. & Trujillo, M. E. Update on the proposed minimal standards for the use of genome data for the taxonomy of prokaryotes. *Int J Syst Evol Microbiol* **74** (2024). https://doi.org:10.1099/ijsem.0.006300

50 Ramasamy, D. *et al.* A polyphasic strategy incorporating genomic data for the taxonomic description of novel bacterial species. *Int J Syst Evol Microbiol* **64**, 384-391 (2014). https://doi.org:10.1099/ijs.0.057091-0

51 Zheng, J. *et al.* A taxonomic note on the genus Lactobacillus: Description of 23 novel genera, emended description of the genus Lactobacillus Beijerinck 1901, and union of Lactobacillaceae and Leuconostocaceae. *Int J Syst Evol Microbiol* **70**, 2782-2858 (2020). https://doi.org:10.1099/ijsem.0.004107

52 Ksiezarek, M., Grosso, F., Ribeiro, T. G. & Peixe, L. Genomic diversity of genus Limosilactobacillus. *Microb Genom* **8** (2022). https://doi.org:10.1099/mgen.0.000847

53 Meziti, A. *et al.* The Reliability of Metagenome-Assembled Genomes (MAGs) in Representing Natural Populations: Insights from Comparing MAGs against Isolate Genomes Derived from the Same Fecal Sample. *Appl Environ Microbiol* **87** (2021). https://doi.org:10.1128/aem.02593-20

54 Valente, C. *et al.* Impact of the 13-valent pneumococcal conjugate vaccine on Streptococcus pneumoniae multiple serotype carriage. *Vaccine* **34**, 4072-4078 (2016). https://doi.org:10.1016/j.vaccine.2016.06.017

55 Kamng'ona, A. W. *et al.* High multiple carriage and emergence of Streptococcus pneumoniae vaccine serotype variants in Malawian children. *BMC Infect Dis* **15**, 234 (2015). https://doi.org:10.1186/s12879-015-0980-2

56 Manenzhe, R. I. *et al.* Characterization of Pneumococcal Colonization Dynamics and Antimicrobial Resistance Using Shotgun Metagenomic Sequencing in Intensively Sampled South African Infants. *Front Public Health* **8**, 543898 (2020). https://doi.org:10.3389/fpubh.2020.543898

57 Turner, P. *et al.* Improved detection of nasopharyngeal cocolonization by multiple pneumococcal serotypes by use of latex agglutination or molecular serotyping by microarray. *J Clin Microbiol* **49**, 1784-1789 (2011). https://doi.org:10.1128/jcm.00157-11

58 Boncoeur, E. *et al.* PatA and PatB form a functional heterodimeric ABC multidrug efflux transporter responsible for the resistance of Streptococcus pneumoniae to fluoroquinolones. *Biochemistry* **51**, 7755-7765 (2012). https://doi.org:10.1021/bi300762p

59 Garvey, M. I., Baylay, A. J., Wong, R. L. & Piddock, L. J. Overexpression of patA and patB, which encode ABC transporters, is associated with fluoroquinolone resistance in clinical isolates of Streptococcus pneumoniae. *Antimicrob Agents Chemother* **55**, 190-196 (2011). https://doi.org:10.1128/aac.00672-10

60 Lupien, A. *et al.* Genomic characterization of ciprofloxacin resistance in a laboratory-derived mutant and a clinical isolate of Streptococcus pneumoniae. *Antimicrob Agents Chemother* **57**, 4911-4919 (2013). https://doi.org:10.1128/aac.00418-13

61 Stogios, P. J. *et al.* Substrate Recognition by a Colistin Resistance Enzyme from Moraxella catarrhalis. *ACS Chem Biol* **13**, 1322-1332 (2018). https://doi.org:10.1021/acschembio.8b00116

62 Lin, J., Wang, Y., Lin, C., Li, R. & Wang, G. High Prevalence of Group III-Like Mutations Among BLPACR and First Report of Haemophilus influenzae ST95 Isolated from Blood in China. *Infect Drug Resist* **16**, 999-1008 (2023). https://doi.org:10.2147/idr.S400207

63 Hood, D. W. *et al.* Three genes, lgtF, lic2C and lpsA, have a primary role in determining the pattern of oligosaccharide extension from the inner core of Haemophilus influenzae LPS. *Microbiology (Reading)* **150**, 2089-2097 (2004). https://doi.org:10.1099/mic.0.26912-0

64 Cardoso, B. *et al.* Genomic insights of international clones of Haemophilus influenzae causing invasive infections in vaccinated and unvaccinated infants. *Microb Pathog* **150**, 104644 (2021). https://doi.org:10.1016/j.micpath.2020.104644

65 Cho, H. E. *et al.* Shotgun Metagenomic Sequencing Analysis as a Diagnostic Strategy for Patients with Lower Respiratory Tract Infections. *Microorganisms* **13** (2025). https://doi.org:10.3390/microorganisms13061338
66 Scott, J. A. *et al.* The definition of pneumonia, the assessment of severity, and clinical standardization in the Pneumonia Etiology Research for Child Health study. *Clin Infect Dis* **54 Suppl 2**, S109-116 (2012). https://doi.org:10.1093/cid/cir1065
67 QIAGEN. *DNeasy® PowerSoil® Kit Handbook*, <https://www.qiagen.com/us/resources/resourcedetail?id=5a0517a7-711d-4085-8a28-2bb25fab828a&lang=en> (2017).
68 QIAGEN. *QIAamp® MinElute®Virus Spin Handbook*, <https://www.qiagen.com/us/products/discovery-and-translational-research/dna-rna-purification/multianalyte-and-virus/qiaamp-minelute-virus-kits> (2020).
69 QIAGEN. *QIAamp DNA Mini and Blood Mini Handbook*, <https://www.qiagen.com/us/products/discovery-and-translational-research/dna-rna-purification/dna-purification/genomic-dna/qiaamp-dna-blood-kits> (March 2024).
70 Espinoza, J. L. & Dupont, C. L. VEBA: a modular end-to-end suite for in silico recovery, clustering, and analysis of prokaryotic, microeukaryotic, and viral genomes from metagenomes. *BMC Bioinformatics* **23**, 419 (2022). https://doi.org:10.1186/s12859-022-04973-8
71 Espinoza, J. L. *et al.* Unveiling the microbial realm with VEBA 2.0: a modular bioinformatics suite for end-to-end genome-resolved prokaryotic, (micro)eukaryotic and viral multi-omics from either short- or long-read sequencing. *Nucleic Acids Res* **52**, e63 (2024). https://doi.org:10.1093/nar/gkae528
72 Chen, S., Zhou, Y., Chen, Y. & Gu, J. fastp: an ultra-fast all-in-one FASTQ preprocessor. *Bioinformatics* **34**, i884-i890 (2018). https://doi.org:10.1093/bioinformatics/bty560
73 Bushnell, B. *BBMap: BBMap short read aligner, and other bioinformatic tools.*, <https://sourceforge.net/projects/bbmap/> (2023).
74 Langmead, B. & Salzberg, S. L. Fast gapped-read alignment with Bowtie 2. *Nat Methods* **9**, 357-359 (2012). https://doi.org:10.1038/nmeth.1923
75 Nurk, S., Meleshko, D., Korobeynikov, A. & Pevzner, P. A. metaSPAdes: a new versatile metagenomic assembler. *Genome Res* **27**, 824-834 (2017). https://doi.org:10.1101/gr.213959.116
76 Kang, D. D. *et al.* MetaBAT 2: an adaptive binning algorithm for robust and efficient genome reconstruction from metagenome assemblies. *PeerJ* **7**, e7359 (2019). https://doi.org:10.7717/peerj.7359
77 Alneberg, J. *et al.* Binning metagenomic contigs by coverage and composition. *Nat Methods* **11**, 1144-1146 (2014). https://doi.org:10.1038/nmeth.3103
78 Wu, Y. W., Simmons, B. A. & Singer, S. W. MaxBin 2.0: an automated binning algorithm to recover genomes from multiple metagenomic datasets. *Bioinformatics* **32**, 605-607 (2016). https://doi.org:10.1093/bioinformatics/btv638
79 Sieber, C. M. K. *et al.* Recovery of genomes from metagenomes via a dereplication, aggregation and scoring strategy. *Nat Microbiol* **3**, 836-843 (2018). https://doi.org:10.1038/s41564-018-0171-1
80 Parks, D. H., Imelfort, M., Skennerton, C. T., Hugenholtz, P. & Tyson, G. W. CheckM: assessing the quality of microbial genomes recovered from isolates, single cells, and metagenomes. *Genome Res* **25**, 1043-1055 (2015). https://doi.org:10.1101/gr.186072.114
81 Shen, W., Le, S., Li, Y. & Hu, F. SeqKit: A Cross-Platform and Ultrafast Toolkit for FASTA/Q File Manipulation. *PLoS One* **11**, e0163962 (2016). https://doi.org:10.1371/journal.pone.0163962
82 Chaumeil, P. A., Mussig, A. J., Hugenholtz, P. & Parks, D. H. GTDB-Tk: a toolkit to classify genomes with the Genome Taxonomy Database. *Bioinformatics* **36**, 1925-1927 (2019). https://doi.org:10.1093/bioinformatics/btz848

83 Sheppard, C. L. *et al.* PneumoKITy: A fast, flexible, specific, and sensitive tool for Streptococcus pneumoniae serotype screening and mixed serotype detection from genome sequence data. *Microb Genom* **8** (2022). https://doi.org:10.1099/mgen.0.000904
84 Epping, L. *et al.* SeroBA: rapid high-throughput serotyping of Streptococcus pneumoniae from whole genome sequence data. *Microb Genom* **4** (2018). https://doi.org:10.1099/mgen.0.000186
85 Watts, S. C. & Holt, K. E. hicap: In Silico Serotyping of the Haemophilus influenzae Capsule Locus. *J Clin Microbiol* **57** (2019). https://doi.org:10.1128/jcm.00190-19
86 Jolley, K. A., Bray, J. E. & Maiden, M. C. J. Open-access bacterial population genomics: BIGSdb software, the PubMLST.org website and their applications. *Wellcome Open Res* **3**, 124 (2018). https://doi.org:10.12688/wellcomeopenres.14826.1
87 Nickols, W. A. *et al.* MaAsLin 3: Refining and extending generalized multivariable linear models for meta-omic association discovery. *bioRxiv* (2024). https://doi.org:10.1101/2024.12.13.628459
88 Rylance, J. *et al.* Household air pollution and the lung microbiome of healthy adults in Malawi: a cross-sectional study. *BMC Microbiol* **16**, 182 (2016). https://doi.org:10.1186/s12866-016-0803-7

Acknowledgements

We acknowledge all participants who contributed samples and their guardians. We also acknowledge the contributions of the laboratory staff at the West Africa Research Platform, Medical Research Council Unit The Gambia at LSHTM, as well as the J. Craig Venter Institute, La Jolla, California

Author contributions

The study was conceived and designed by MPN, BKA, MA and CLD. Data analysis was conducted by DK and JLE. Figures were prepared by DK. DK wrote the initial draft of the Manuscript. MPN, CLD, BKA, MA, IDO and JLE edited and revised the manuscript. All authors participated in the discussion and interpretation of the results.

Data Availability

Shotgun metagenomic sequencing data has been deposited in the NCBI Sequence Read Archive (SRA) associated with BioProject PRJNA727021. The accession numbers of the 71 samples used in the analysis in this paper are detailed in Supplementary Table S3. The 35 high-quality MAGs reported in this paper, together with the analysis scripts and supporting files are made available in Zenodo at https://zenodo.org/records/22771565.

Funding

This work is supported by the U.S. National Institutes of Health (NIH), Office of the Director (OD), the National Institute of Environmental Health Sciences (NIEHS), and the National Human Genome Research Institute (NHGRI) grant number U54HG009824.

Additional information

The authors declare no competing interests

Figure legends

Figure 1: List of specimen type analysed for each of the 37 participants. Rows represent individual participants, ordered by shared sample availability profiles to visually group individuals with identical patterns of missing or available sample.

Figure 2: (a) Prevalence of AMR genes in all 35 high-quality MAGs. Bars are coloured according to antibiotic class of each corresponding gene. (b) AMR genes detected in the high-quality MAGs grouped by specimen type. The y-axis of each plot lists all AMR genes detected within that specimen type. The AMR gene names are coloured according to their antibiotic class. MLS: Macrolide-Lincosamide-Streptogramins. Nm: *Neisseria meningitidis,* Hi: *Haemophilus influenzae*, Ls: *Limosilactobacillus Sp*. Ml: *Moraxella lincolnii,* Mc: *Moraxella catarrhalis,* Sp: *Streptococcus pneumoniae,* Mn: *Moraxella nonliquefaciens,* Hp: *Haemophilus parahaemolyticus*

Figure 3: Barplots of the compositional mean relative abundances of bacteria DNA at the phylum (a) and species (b) levels. All six phyla detected in our dataset are shown in the phylum-level plot. The Top 14 bacterial species is shown in the species-level plot. All remaining species were grouped as "Other". The top 14 species were identified based on the sum of their compositional relative

878 abundances across all specimen type. Specimen type is shown on the y-axis, and the compositional
879 mean relative abundance of each taxonomic group is shown on the x-axis. The number of samples
880 (equal to the number of participating individuals contributing each specimen type) is indicated in
881 parantheses on the bar labels. DNA extraction methods for each specimen type: DNeasy PowerSoil
882 Kit (NPS, NP-OP, IS), QIAamp MinElute Virus Spin Kit (LA), and QIAamp DNA Blood Mini Kit (blood).
883 NPS: nasopharyngeal swab, NP-OP: nasopharyngeal/oropharyngeal swab, IS: induced sputum, LA:
884 lung aspirate

885 Figure 4: Shannon diversity of bacterial communities by specimen type. The horizontal line within
886 each box represents the median Shannon diversity, while the upper and lower bounds of each
887 boxplot represent the 75% and 25% quartiles. Pairwise comparisons were performed using a linear
888 mixed-effects model with participant as a random intercept, followed by Tukey's post-hoc adjustment
889 for multiple comparisons. Significant differences between specimen types are indicated by asterisks
890 (* $p < 0.05$, ** $p < 0.01$, *** $p < 0.001$). The number of samples (equal to the number of participating
891 individuals contributing each specimen type) is indicated in parentheses on the x-axis labels. DNA
892 extraction methods: DNeasy PowerSoil Kit (NPS, NP-OP, IS), QIAamp MinElute Virus Spin Kit (LA), and
893 QIAamp DNA Blood Mini Kit (blood). NPS: nasopharyngeal swab, NP-OP:
894 nasopharyngeal/oropharyngeal swab, IS: induced sputum, LA: lung aspirate.

895 Figure 5: Mean Jaccard similarity index (%) of bacterial species detected in paired blood and
896 respiratory specimens from the same participants. Error bars represent standard error of the mean.
897 Number of participant pairs is shown in parentheses on the x-axis. Asterisk indicates a permutation
898 test $p < 0.05$ comparing observed within-participant Jaccard similarity against a null distribution
899 generated from 9,999 random reassignments of paired samples. "ns" indicates $p > 0.05$.

900 Figure 6: Barplots of the compositional mean relative abundances of bacterial DNA at the species
901 level in the nasopharynx (NPS) of severe and very severe cases. Case type is shown on the Y-axis, and
902 the relative abundance of each species is shown on the X-axis. Taxa that are not in the top 14 most

903 abundant species are aggregated under "Other". The number of samples included in each category is
904 added in the bar labels.

905

906 Table 1: Demographic and clinical characteristics of children. This table includes all children who
907 contributed at least one specimen to any analysis.

	Classification	Frequency (%)
Sex	Male	22 (59)
	Female	15 (41)
Age	1-5 months	15 (41)
	6-11 months	4 (11)
	12-23 months	8 (22)
	24-59 months	10 (27)
Hib vaccination status	Not vaccinated	6 (16)
	Partially vaccinated	9 (24)
	Fully vaccinated	20 (54)
	No data	2 (5)
PCV vaccination status	Not vaccinated	8 (22)
	Partially vaccinated	8 (22)
	Fully vaccinated	19 (51)
	No data	2 (5)
Pneumonia severity	Severe	16 (43)
	Very severe	21 (57)
HIV status	Positive	2 (5)
	Negative	31 (84)

	Unconfirmed	4 (11)

908

909

910 Table 2: Characterisation of high-quality metagenome-assembled genomes obtained from blood and

911 respiratory samples

	Species	ANI with type strain (%)	Number of contigs	N50	Genome Size (Mb)	Completeness (%)	Contamination (%)	Strain heterogeneity	Source specimen
MAG1	*Neisseria meningitidis*	97.58	227	11345	1.80	95.79	0.23	0	NP-OP
MAG2	*Haemophilus parahaemolyticus*	97.3	146	17420	1.78	90.94	1.24	66.67	IS
MAG3	*Moraxella catarrhalis*	99.12	273	8974	1.75	92.31	1.38	22.22	IS
MAG4	*Streptococcus pneumoniae*	98.53	114	26698	2.00	98.5	0	0	LA
MAG5	*Moraxella catarrhalis*	99.08	69	38190	1.77	95.76	0.42	33.33	NP-OP
MAG6	*Streptococcus pneumoniae*	98.62	69	44339	2.16	99.63	0.06	0	NP-OP
MAG7	*Haemophilus influenzae*	97.17	96	50042	1.92	99.37	0.25	50	IS
MAG8	*Haemophilus parahaemolyticus*	97.24	265	9977	1.83	90.75	1.05	28.57	IS
MAG9	*Streptococcus pneumoniae*	98.63	244	11618	1.80	93.6	0.41	20	NPS
MAG10	*Haemophilus influenzae*	97.14	56	93732	1.84	99.55	0.76	16.67	LA
MAG11	*Streptococcus pneumoniae*	99.52	76	67168	2.02	99.63	0	0	LA
MAG12	*Moraxella catarrhalis*	96.14	175	28060	2.00	97.56	3.54	10.53	LA
MAG13	*Haemophilus influenzae*	97.49	247	11400	1.83	92.84	3.45	56.52	LA
MAG14	*Streptococcus pneumoniae*	98.6	88	32376	2.05	99.63	0	0	Blood
MAG15	*Haemophilus influenzae*	97.39	167	20433	1.63	91.37	0.8	100	NP-OP
MAG16	*Streptococcus pneumoniae*	98.57	87	39492	2.07	99.44	0	0	LA
MAG17	*Haemophilus influenzae*	97.1	60	71164	1.80	98.98	0	0	LA
MAG18	*Haemophilus influenzae*	97.38	29	122554	1.79	99.55	0	0	LA
MAG19	*Haemophilus influenzae*	98.8	22	137938	1.85	99.66	0.23	0	Blood
MAG20	*Streptococcus pneumoniae*	98.45	197	16266	2.01	97.44	1.07	0	Blood
MAG21	*Moraxella catarrhalis*	99.23	139	28747	1.94	97.29	0.63	75	Blood
MAG22	*Moraxella catarrhalis*	99.12	26	120380	1.85	99.45	1.07	14.29	Blood
MAG23	*Streptococcus pneumoniae*	98.65	62	45294	2.08	99.63	0	0	Blood

MAG24	*Haemophilus influenzae*	97.11	26	186272	1.86	99.55	0	0	Blood
MAG25	*Limosilactobacillus Sp.*		228	8961	1.50	97.81	0.13	0	NP-OP
MAG26	*Neisseria meningitidis*	97.61	158	18553	1.97	99.18	0.38	0	Blood
MAG27	*Streptococcus pneumoniae*	98.56	64	48015	2.12	99.63	0	0	Blood
MAG28	*Moraxella nonliquefaciens*	98.47	56	343360	2.28	96.85	3.48	0	Blood
MAG29	*Haemophilus influenzae*	97.21	157	29106	1.93	95.55	1.05	28.57	Blood
MAG30	*Moraxella catarrhalis*	99.08	65	74719	1.98	98.88	0.44	25	NPS
MAG31	*Haemophilus influenzae*	97.28	156	19152	1.75	98.05	0.84	40	NPS
MAG32	*Streptococcus pneumoniae*	98.59	339	6926	1.83	91.90	1.37	83.33	NPS
MAG33	*Moraxella lincolnii*	97.95	243	13659	2.07	92.60	0.5	66.67	NP-OP
MAG34	*Streptococcus pneumoniae*	98.86	238	10781	1.90	94.76	0.75	50	NPS
MAG35	*Moraxella nonliquefaciens*	98.22	103	57578	2.34	95.75	4.84	6.06	NPS

912

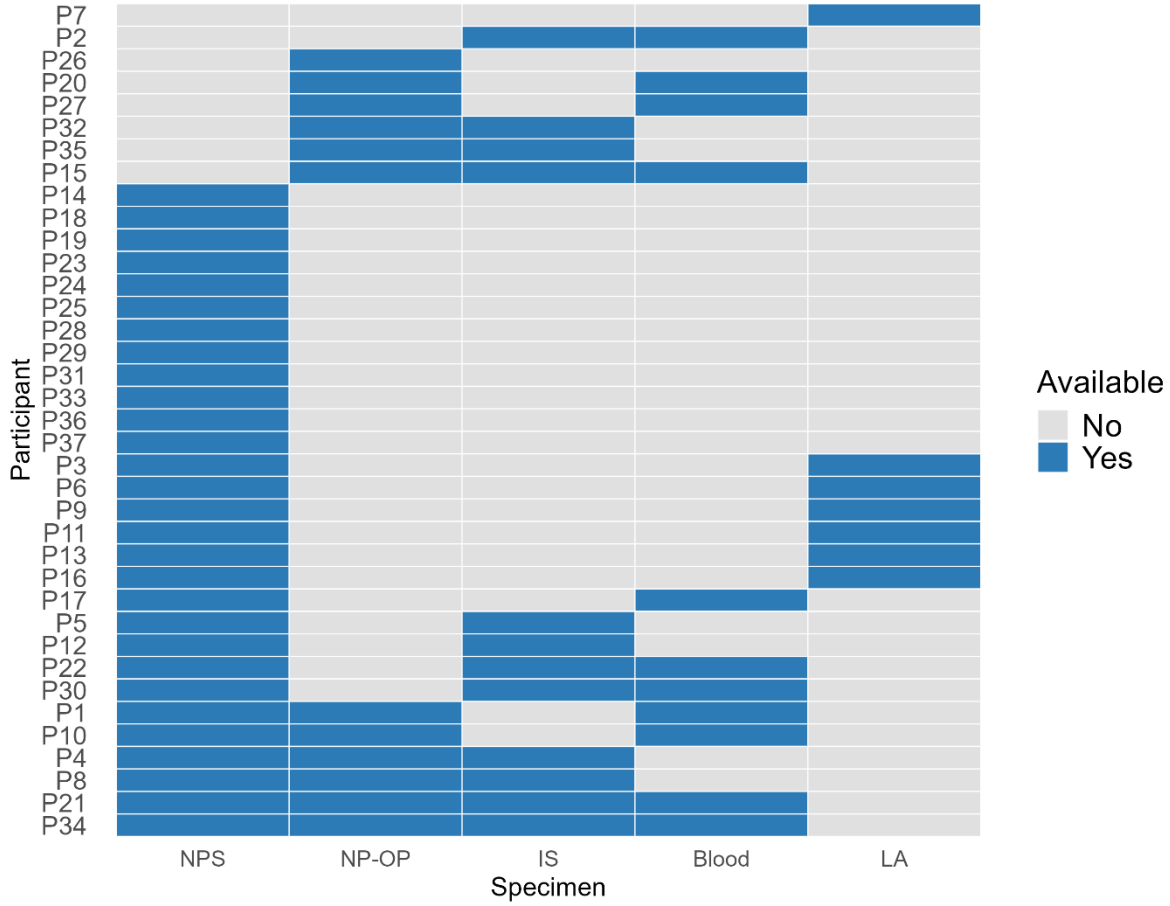

913

914 Figure 1

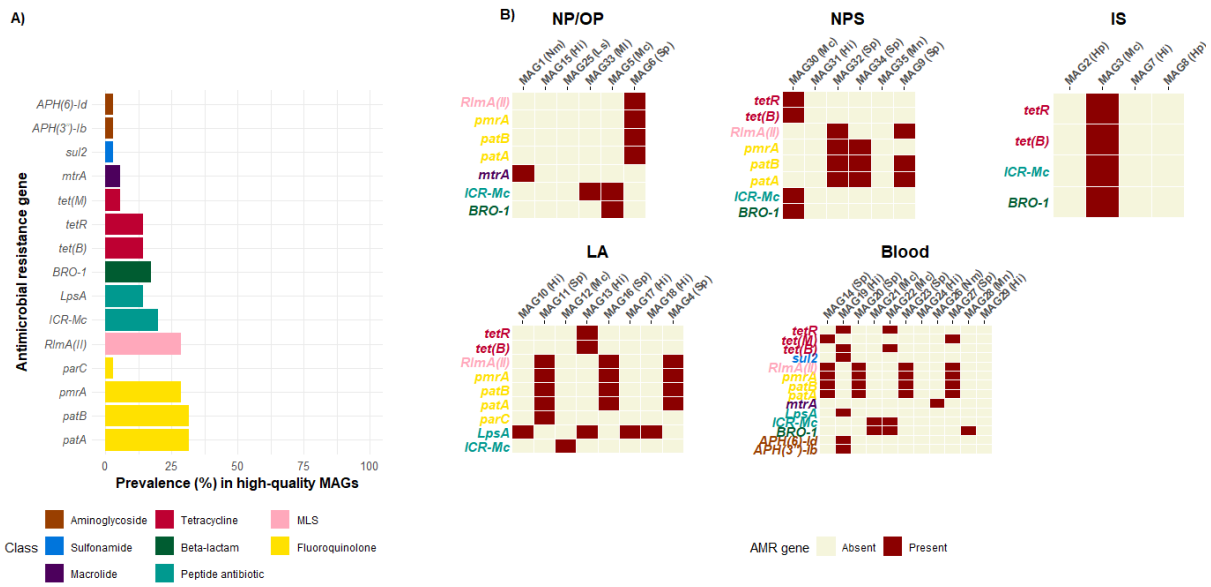

915

916 Figure 2

917

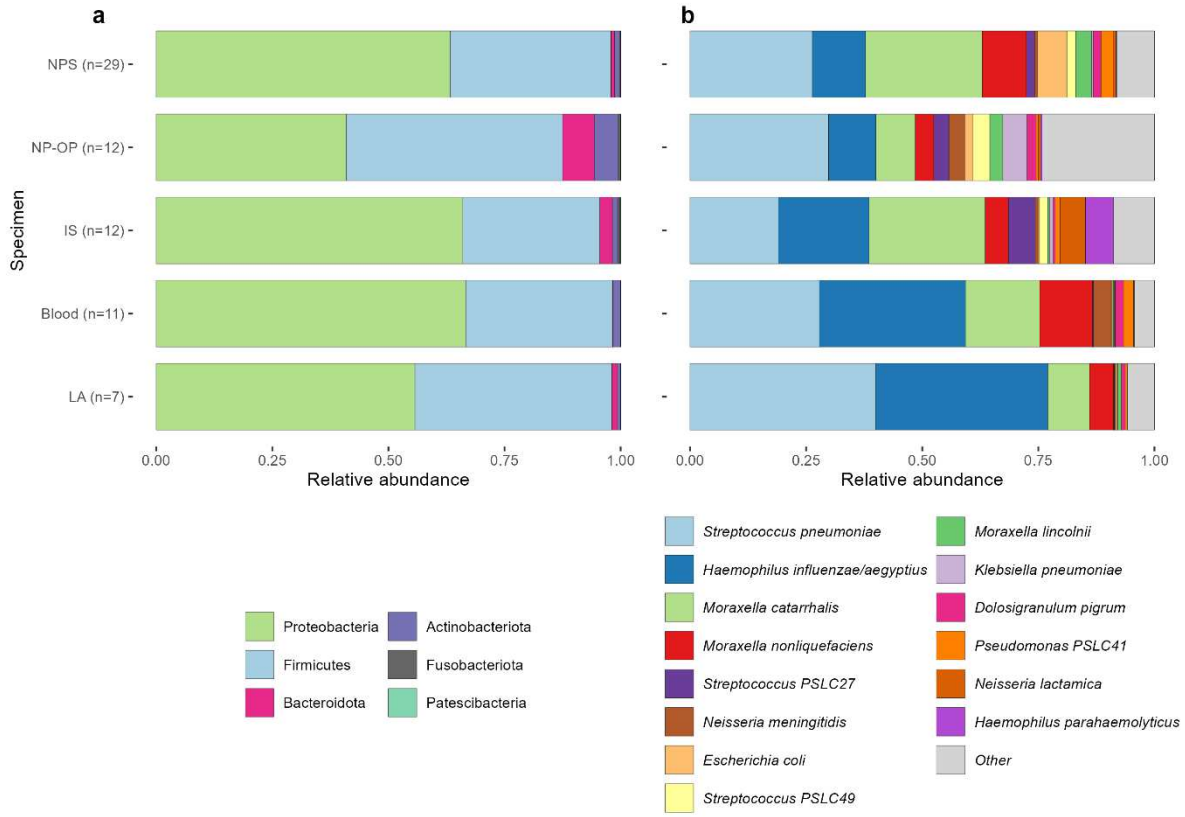

918

919 Figure 3

920

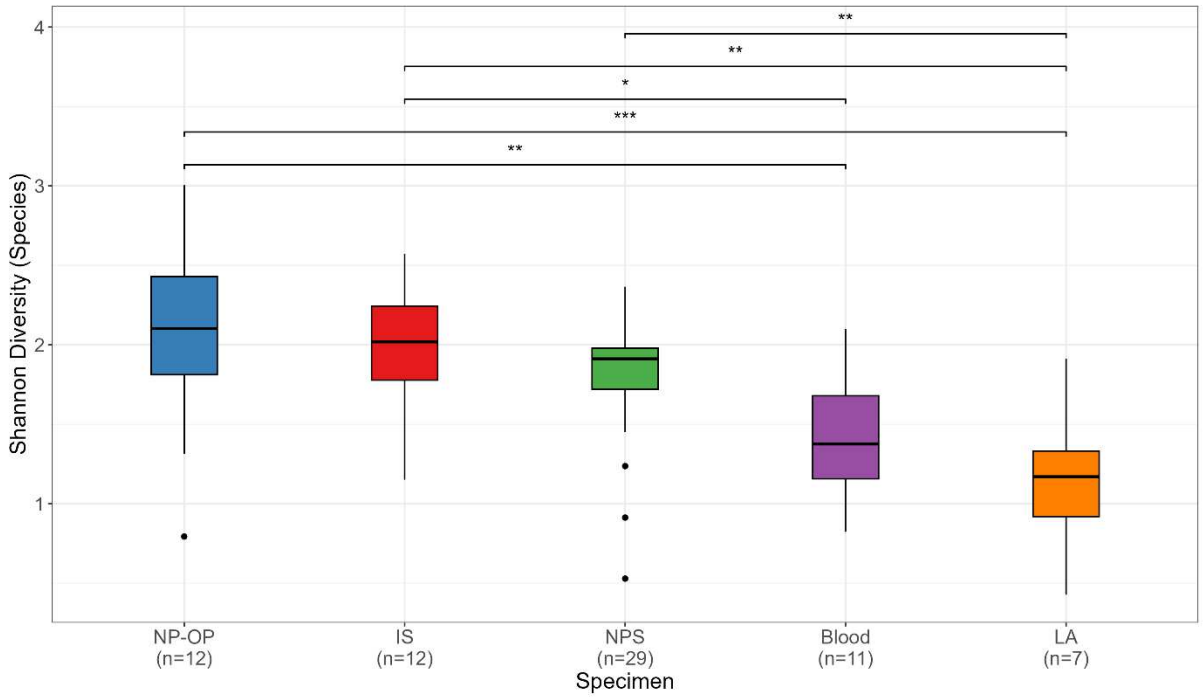

921

922 Figure 4

923

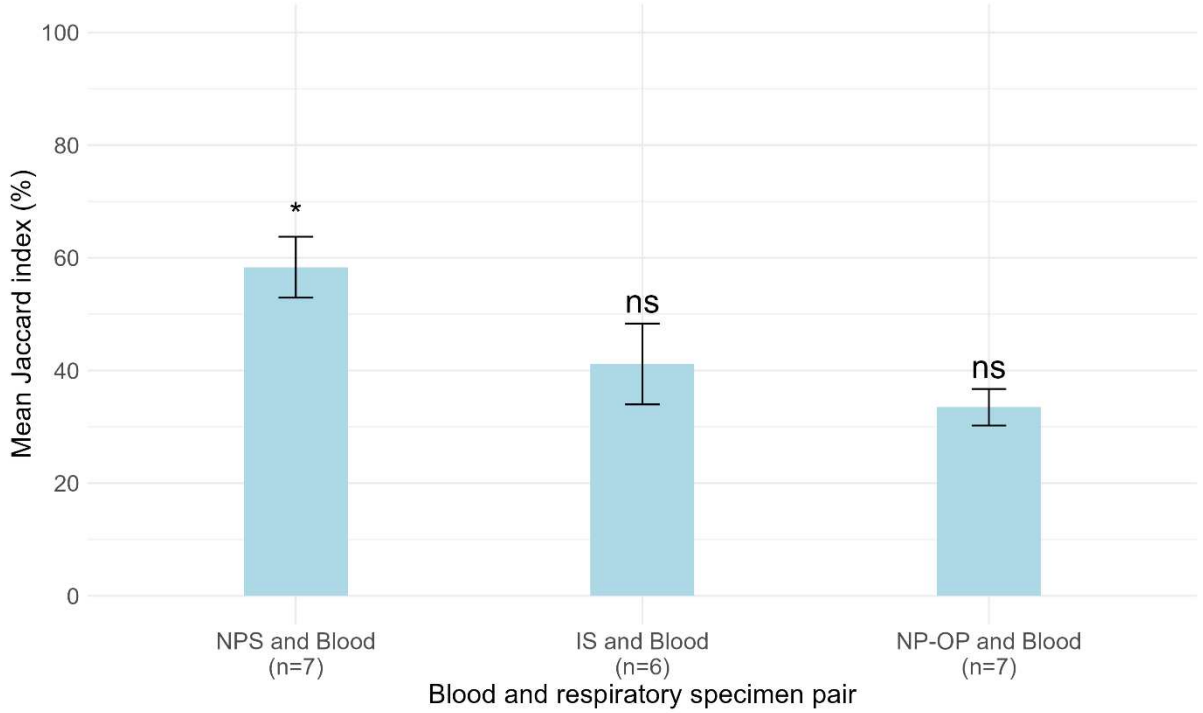

924

925 Figure 5

926

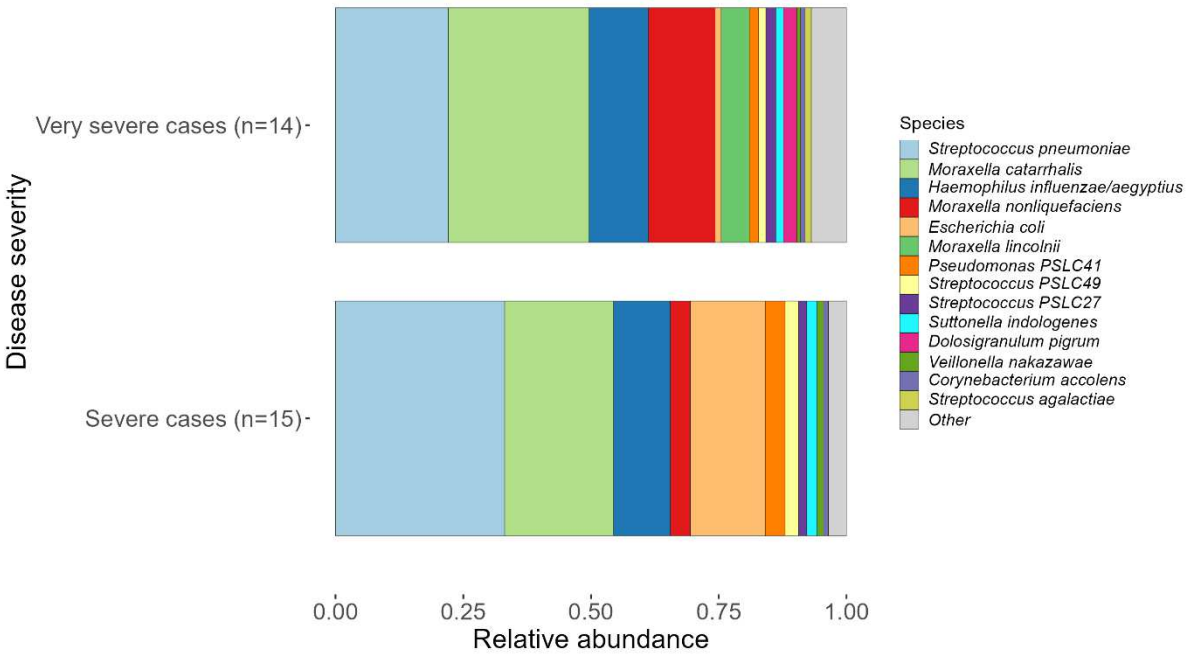

927

928 Figure 6

929

930

931

Supplementary Files

This is a list of supplementary files associated with this preprint. Click to download.

- Supplemetaryinformationclean.pdf